0090-9556/07/3511-2127–2137$20.00
DRUG METABOLISM AND DISPOSITION
Vol. 35, No. 11
16840/3260429
Printed in U.S.A.

DMD 35:2127–2137, 2007

Serine Hydroxymethyltransferase Isoforms Are Differentially Inhibited by Leucovorin: Characterization and Comparison of Recombinant Zebrafish Serine Hydroxymethyltransferases

Wen-Ni Chang, Jen-Ning Tsai, Bing-Hung Chen, Huei-Sheng Huang, and Tzu-Fun Fu

Department of Medical Laboratory Science and Biotechnology, College of Medicine, National Cheng Kung University, Tainan, Taiwan (W.-N.C., H.-S.H., T.-F.F.); School of Medical Laboratory and Biotechnology, Chung Shan Medical University, Taichung, Taiwan (J.-N.T.); and Faculty of Biotechnology, Kaohsiung Medical University, Kaohsiung, Taiwan (B.-H.C.)

Received May 24, 2007; accepted July 25, 2007

ABSTRACT:

Serine hydroxymethyltransferase (SHMT) provides activated one-carbon units required for the biosynthesis of nucleotides, protein, and methyl group by converting serine and tetrahydrofolate to glycine and N^5,N^{10}-methylenetetrahydrofolate. It is postulated that SHMT activity is associated with the development of methotrexate resistance and the in vivo activity of SHMT is regulated by the binding of N^5-CHO-THF, the rescue agent in high-dose methotrexate chemotherapy. The aim of this study is to advance our understanding of the folate-mediated one-carbon metabolism in zebrafish by characterizing zebrafish mitochondrial SHMT. The cDNA encoding zebrafish mitochondrial SHMT was cloned, overexpressed in *Escherichia coli*, and purified with a three-step purification protocol. Similarities in structural, physical, and kinetic properties were revealed between the recombinant zebrafish mitochondrial SHMT and its mammalian orthologs. Surprisingly, leucovorin significantly inhibits the aldol cleavage of serine catalyzed by zebrafish cytosolic SHMT but inhibits to a lesser extent the reaction catalyzed by the mitochondrial isozyme. This is, to our knowledge, the first report on zebrafish mitochondrial folate enzyme as well as the differential inhibition of leucovorin on these two SHMT isoforms. Western blot analysis revealed tissue-specific distribution with the highest enrichment present in liver for both cytosolic and mitochondrial SHMTs. Intracellular localization was confirmed by confocal microscopy for both mitochondrial and cytosolic SHMTs. Unexpectedly, the cytosolic isoform was observed in both nucleus and cytosol. Together with the previous report on zebrafish cytosolic SHMT, we suggest that zSHMTs can be used in in vitro assays for folate-related investigation and antifolate drug discovery.

Folates carry the chemically activated single carbons at N^5 and/or N^{10} positions and are required for the biosynthesis and metabolism of nucleic acid, protein, amino acid, methyl group, neurotransmitter, and vitamins. Its vital role in nucleotide biogenesis has led to the development of many anticancer drugs targeting folate-requiring enzymes. Among them, methotrexate (MTX) is one of the most widely used anticancer agents to date. It blocks de novo nucleotide synthesis by depleting reduced tetrahydrofolates mainly through inhibition of dihydrofolate reductase (DHFR) and thymidylate synthase (Fig. 1, enzymes 2 and 3, respectively). However, resistance to MTX often emerges and becomes the major impediment to its curative potential. To overcome this obstacle and prevent MTX-associated toxicity, high-dose MTX combined with leucovorin rescue is administered and has become an important regimen in the treatment of a variety of cancers (Frei et al., 1980). Despite these preventive measures, MTX-induced resistance and toxicity continue to occur, although infrequently. Mechanisms including elevated DHFR, decreased thymidylate synthase, impaired folate/antifolate transportation, and decreased polyglutamylation on MTX have been proposed to contribute to the development of MTX resistance (Asai et al., 2003). It is also postulated that the excessive use of leucovorin makes tumor cells refractory to subsequent MTX therapy (Bleyer, 1977; Sirotnak et al., 1978). Nevertheless, what causes the emergence of MTX-resistant tumor cells and the reason why high concentrations of leucovorin might affect cell survival or even support MTX resistance remain to be answered.

In vivo, N^5-CHO-THF, also known as leucovorin, is generated by the irreversible hydrolysis of N^5,N^{10}-CH^+-THF in a second reaction

This work was supported by Grant NSC 95-2320-B-006-022 from the National Science Council, Taiwan.

W.N.C. and T.F.F. contributed equally to this work.

Article, publication date, and citation information can be found at http://dmd.aspetjournals.org.

doi:10.1124/dmd.107.016840.

ABBREVIATIONS: MTX, methotrexate; SHMT, serine hydroxymethyltransferase; zmSHMT and zcSHMT, zebrafish mitochondrial and zebrafish cytosolic SHMT; hcSHMT and rcSHMT, human cytosolic and rabbit cytosolic enzymes; THF or H_4PteGlu, tetrahydropteroylglutamate; N^5-CHO-H_4PteGlu, N^5-formyl-tetrahydropteroylglutamate; N^5,N^{10}-CH_2-, N^5,N^{10}-methylene; N^5-CH_3-, N^5-methyl; PLP, pyridoxal-5′-phosphate; DHFR, dihydrofolate reductase; RT-PCR, reverse transcription-polymerase chain reaction; EGFP, enhanced green fluorescent protein; IPTG, isopropyl-β-D-thiogalactopyranoside; PAGE, polyacrylamide gel electrophoresis; PVDF, polyvinylidene difluoride; ZLE, zebrafish liver epithelial; RACE, rapid amplification of cDNA ends; UPM, Universal Primer Mix; NUP, Nested Universal Primer; bp, base pair(s); kb, kilobase(s); (F), forward; (R), reverse; GFP, green fluorescent protein; SUMO, small ubiquitin-like modifier.

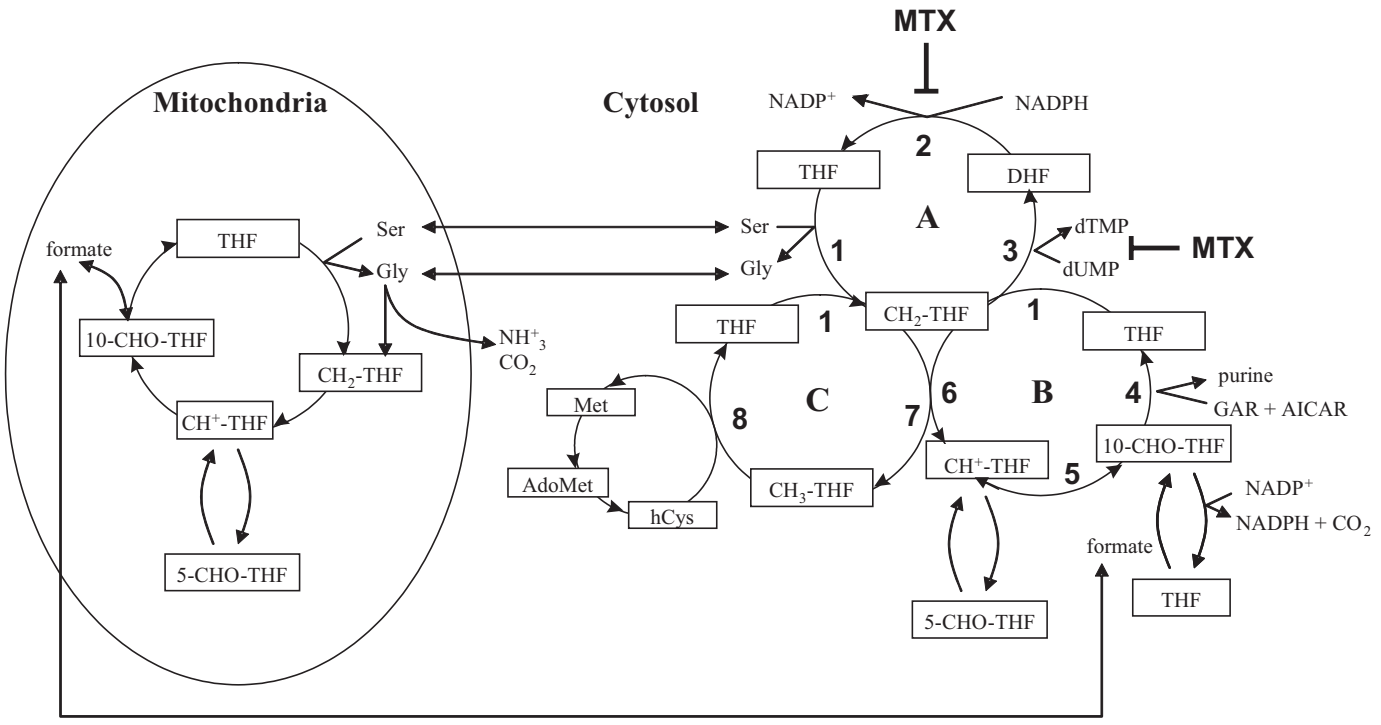

FIG. 1. The folate-mediated one-carbon metabolism involving both cytosolic and mitochondrial serine hydroxymethyltransferases. Folate coenzymes are equally distributed in cytosolic and mitochondrial compartments. Three cycles are involved in this pathway and are responsible for thymidylate (A), purine (B), and methionine biosynthesis (C). The enzymes participating in this pathway are serine hydroxymethyltransferase (1), dihydrofolate reductase (2), thymidylate synthase (3), glycinamide ribonucleotide transformylase (GAR) and 5-amino-4-imidazolecarboxamide ribotide transformylase (AICAR) (4), N^5,N^{10}-methenyltetrahydrofolate cyclohydrolase (5), N^5,N^{10}-methylenetetrahydrofolate dehydrogenase (6), N^5,N^{10}-methylenetetrahydrofolate reductase (7), and methionine synthase (8). A parallel pathway also exists in mitochondria, where the activated one-carbon unit is generated in the serine-aldol cleavage catalyzed by mitochondrial serine hydroxymethyltransferase.

catalyzed by serine hydroxymethyltransferase (SHMT). N^5-CHO-THF also acts as a tight-binding inhibitor of the cytosolic form of SHMT (Stover and Schirch, 1991). SHMT is a pyridoxal-5′-phosphate (PLP)-dependent enzyme and reversibly converts serine and THF to glycine and N^5,N^{10}-CH_2-THF, the principal pathway of one-carbon unit incorporation in cells. One-carbon metabolism is compartmentalized with folate coenzymes equally distributed in cytosol and mitochondria (Appling, 1991). In higher organisms more than one SHMT isoform is often present: a cytosolic isoform and an organelle-associated form, usually mitochondria. Although the physiological functions of these two isozymes remain unclear, it is suggested that cytosolic SHMT (cSHMT) tends to function in the direction of serine synthesis, whereas the production of glycine and N^5,N^{10}-CH_2-THF is mainly catalyzed by mitochondrial SHMT (mSHMT) (Narkewicz et al., 1996). Studies suggested that the activity of cSHMT is associated with the development of MTX resistance. It is believed that the cSHMT activity in vivo is modulated by the binding of N^5-CHO-THF and functions as a metabolic switch that shuttles the one-carbon unit between dTMP biosynthesis and homocysteine remethylation (Herbig et al., 2002). Yet the effect of N^5-CHO-THF on mSHMT activity and the importance of mSHMT in leucovorin metabolism and MTX resistance remain undetermined, even though the uptake of N^5-CHO-THF by mitochondria has been shown to be rapid and concentration-dependent (Horne et al., 1992). Currently, the animal model used for folate-related studies is restricted mostly to rodent for its resemblance with human in folate-requiring enzymes. However, deciphering the role of folate enzymes in early mammalian development might be limited because of the maternal contribution of folate coenzymes during embryogenesis (Marasas et al., 2004). Considering the feature of external development, zebrafish might serve as a valuable alternative for folate-related studies since the maternal supply of folates and folate enzymes is likely to be depleted with time in developing embryos. Increasing studies also demonstrate comparable features between zebrafish and human in many biological pathways and pathogenesis, including organ development, angiogenesis, hemostasis, heart function and circulation, apoptosis and proliferation, carcinogenesis, drug abuse and addiction, and toxicology and teratogenicity (Kari et al., 2007). However, folate-requiring one-carbon metabolism in zebrafish remains unexplored territory, albeit its critical role in oncogenesis and fetal development in vertebrates.

Our previous study on the recombinant zebrafish cSHMT revealed strong similarities with mammalian orthologs, suggesting the appropriateness of using zebrafish as a model for folate-related studies (Chang et al., 2006). In the present report, we clone and characterize zebrafish mitochondrial SHMT (zmSHMT), the other isoform of SHMT, which is less understood in mammals. To our knowledge, this is the first report on a mitochondrial folate enzyme from zebrafish that is successfully expressed and purified in *Escherichia coli*. The similarities revealed between zebrafish mSHMT and human orthologs add more confidence to the uses of zebrafish in folate-related studies and drug discovery. In addition, we observe differential inhibition mediated by MTX and leucovorin on the catalytic activity of these two isoforms. The potential contribution of this observation to the development of MTX resistance is also discussed.

Materials and Methods

Materials. Polymerase chain reaction (PCR) primers were ordered from MDBio, Inc. (Taipei, Taiwan). The SMART RACE Amplification Kit was purchased from Clontech, Inc. (Mountain View, CA). PCR Master Mix was purchased from ABgene House (Epsom, Surrey, UK). Restriction enzymes used for cloning procedures were purchased from either Invitrogen (Carlsbad, CA) or New England BioLabs (Ipswich, MA). The clone expressing rabbit

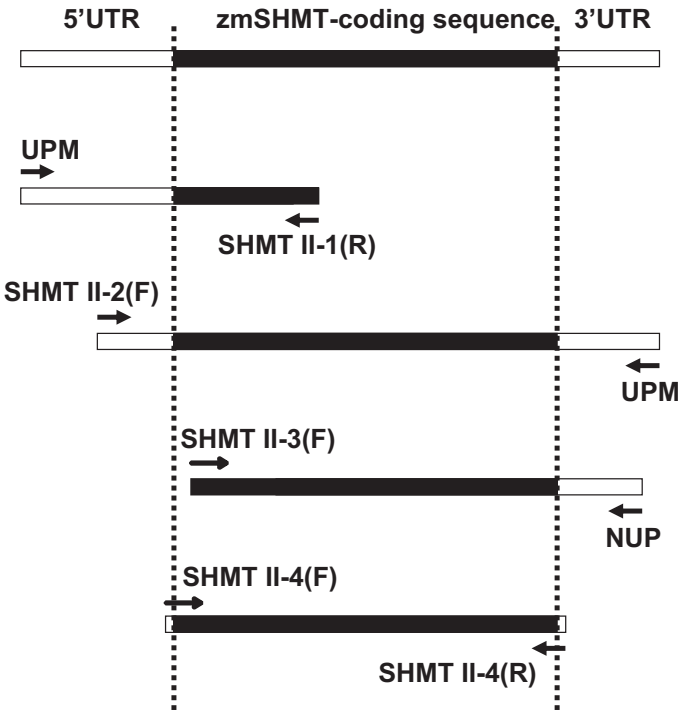

SCHEME 1. PCR-based cloning of mitochondrial SHMT from the first-strand RACE-cDNA library prepared from 24-hr zebrafish embryos. The cloning was accomplished following the procedures described under *Materials and Methods*.

N^5,N^{10}-methylenetetrahydrofolate dehydrogenase was a generous gift from Dr. Verne Schirch (Virginia Commonwealth University, Richmond, VA). The HPLC gel filtration column Alltech ProSphere SEC, 250 HR, *S*-200 (4.6 mm × 30.0 cm) was purchased from Alltech Associates (Deerfield, IL). (6*S*)-Tetrahydrofolate monoglutamate and (6*S*)-N^5-CHO-tetrahydrofolate monoglutamate were generous gifts from Dr. R. Moser (Merck Eprova AG, Schaffhausen, Switzerland). Mitotracker Red probes for confocal microscopy were purchased from Invitrogen. Polyvinylidene difluoride (PVDF) membranes were purchased from Millipore Corporation (Billerica, MA). Both the Bradford assay reagent and BCA protein assay kit were purchased from Pierce (Rockford, IL). Rabbit polyclonal anti-zcSHMT antibodies were produced by Genesis Biotech Inc. (Hsintein, Taiwan), with the enzymes we provided. Goat anti-hmSHMT antibodies, horseradish peroxidase-conjugated goat anti-rabbit IgG, and donkey anti-goat secondary antibody were purchased from Santa Cruz Biotechnology Inc. (Santa Cruz, CA). The zebrafish liver epithelial cell line ZLE, established by C. L. Miranda, P. Collodi, X. Zhao, D. W. Barnes, and D. R. Buhler, was generously provided by Dr. Jiann-Ruey Hong (National Cheng Kung University, Tainan, Taiwan). All other chemicals, including coenzymes, buffers, amino acids, and antibiotics, were purchased from Sigma-Aldrich (St. Louis, MO).

Fish Care and Preparation of cDNA Library from Zebrafish Embryos. Zebrafish (*Danio rerio*, AB strain) were bred and maintained in a 14 h/10 h light-dark diurnal cycle according to the standard condition described by Westerfield (2000). Embryos were staged according to the method of Kimmel et al. (1995). Total RNA isolation and cDNA library construction from zebrafish embryos were performed with RNAzol B reagent (Tel-Test Inc., Friendswood, TX) and the SMART RACE cDNA Amplification Kit (Clontech, Inc.) as described previously (Chang et al., 2006).

Bacterial Strains, Plasmids, and General Cloning Procedures. The *E. coli* strain XL1 Blue (*rec*A1, *end*A1, *gyr*A96, *thi-1*, *hsd*R17(r_K^- m_K^+) (*sup*E44, *rel*A1, *lac*$^-$) was used for the construction of clones. The *E. coli* strains HMS174(DE3) (F^- recA r_{k12}^- m_{k12}^+) and Rosetta (DE3) (F^- recA r_{k12}^- m_{k12}^+), which contain the T7 RNA polymerase gene, were used for protein expression. The pET43.1a plasmid and all the *E. coli* strains for cloning and expression were obtained from Novagen (Madison, WI). The materials and methods for the general cloning procedures were as described previously (Chang et al., 2006).

Cloning of zmSHMT from Zebrafish cDNA Library by PCR-Based Cloning Strategy. A PCR-based approach with degenerate primers was used for the amplification and cloning of SHMT-encoding sequences from a zebrafish cDNA mixture. Two degenerate primers (5′-TGGGGNGTNAAYGTNCA-3′ and 5′-WDATRTGNGCCATRTC-3′), corresponding to the conserved regions of SHMT amino acid sequences (WGVNVQ and DMAHIS), were designed for PCR with the following conditions: a denaturation of 94°C for 5 min followed by 55 cycles of 94°C for 30 s, 60°C for 30 s, and 72°C for 90 s. The resultant products were cloned and sequenced. The deduced amino acid sequences of the amplified products fell into two categories and shared 70 to 90% identity with the corresponding regions of SHMT. GenBank BLAST search revealed 100% and 61% identity between these two sequences and zcSHMT cDNA (zebrafish *shmt1*, accession number NM_201046). Based on the sequence information of the 61% identity fragment, we proceeded with the isolation of prospective zebrafish mitochondrial SHMT cDNA.

The cloning of full-length zmSHMT cDNA was accomplished by the rapid amplification of cDNA ends (RACE) method using zmSHMT gene-specific primers designed on the basis of the sequence information of the cloned fragment (Scheme 1). The reverse primer SHMT II-1(R) (5′-AGCGATGATGAGTTTGGGTCTGAA-3′) and the UPM primer provided in the SMART RACE cDNA Amplification Kit (Clontech, Inc.) were used in the first-round PCR, with the 5′RACE cDNA mixture as template. The resultant bands were TA-cloned and sequenced. Based on the sequence information, two primers, SHMT II-2(F) (5′-AGAGTACGGGGGGGCTGTCATTTA-3′) and SHMT II-3(F) (5′-TGCTGACACTGACATTACGACAAA-3′) were designed for subsequent PCR amplifications. The SMART 3′-RACE cDNA mixture was used as template in the second-round PCR with primer pairs SHMT II-2(F) and UPM. The third round of PCR was conducted using the second-round PCR product as template and the primer pairs SHMT II-3(F) and NUP provided in the kit. All of the above amplifications were performed by touchdown PCR. The cycling conditions were 5 cycles of 94°C for 30 s and 72°C for 3 min; 5 cycles of 94°C for 30 s, 70°C for 30 s, and 72°C for 3 min; 40 cycles of 94°C for 30 s, 68°C for 30 s, and 72°C for 3 min. The resulting 2700-bp fragment was identified by restriction mapping and sequencing. The assembling of 5′-RACE and 3′-RACE sequences revealed the prospective full-length zmSHMT cDNA. The final amplification of the complete 1.5-kb encoding sequence was accomplished by PCR with the 5′-RACE cDNA library prepared from 3-day post-fertilization embryos as template and the primer pair SHMT II-4(F), 5′-CCGGATCCATATGCTGACACTGACATTACG-3′ (forward) and SHMT II-4(R), 5′-CCCTGATGAATTCGTTTAATGGTCGTGGAATCC-3′ (reverse). To simplify the cloning procedure, two restriction enzyme sites, NdeI and EcoRI (underlined), were introduced into the primers. The PCR-amplified product was cloned into the expression vector pET43.1a.

Successful cloning was confirmed by both restriction enzyme digestion and DNA sequencing.

Removal of signal peptide and introduction of the first methionine residue was accomplished by PCR using zmSHMT coding sequence as template with the primer pair 5′-GCGCTCCTCCCATATGGTGTGTGTGCGC-3′ (forward) and SHMT II-4 (reverse) followed by cloning into the pET43.1a vector, yielding the clone zmSHMT(DelSig). The resultant constructs were transformed into an *E. coli* host cell Rosetta (DE3) for enzyme expression and purification.

Zebrafish SHMT-EGFP fusion plasmids were constructed by PCR cloning with the zcSHMT or zmSHMT plasmids and the primers designed to abolish stop codons and introduce BglII, EcoRI, or SalI restriction enzyme sites. The primers were 5′- GCGTTGGGAGATCTCCCATATG-3′ (forward) and 5′-CAAGCAGAAATGAATTCGTAACTCTGGCAACC-3′ (reverse) for zcSHMT/pEGFP-N1; 5′-GCGTTGGGAGATCTCCCATATG -3′ (forward) and 5′-CCGCGGGAATTCGTCGACTGGTCGTGGAATCC-3′ (reverse) for zmSHMT/pEGFP-N1.

Expression and Purification of Recombinant zmSHMT. All buffers described below for the purification of zSHMTs and kinetic studies contained 5 mM 2-mercaptoethanol, 0.2 mM EDTA, and 2 μM PLP unless otherwise stated. Similar purification procedures for zcSHMT were applied to the purification of zmSHMT(DelSig) with minor modifications indicated below (Chang et al., 2006). In brief, *E. coli* containing the desired plasmid was grown to log phase and enzyme-induced at 25°C with 0.08 mM IPTG for 3 h. Cells were harvested and lysed with lysozyme and chromatin was removed by protamine sulfate precipitation. After a 30% to 50% ammonium sulfate fractionation and desalting on a P-6DG column, zmSHMT(DelSig) was loaded onto a CM-Sephadex column (2.5 × 5.0 cm) and eluted with the linear salt gradient of 50 ml of equilibrating buffer and 50 ml of 500 mM potassium phosphate, pH 7.25. The purified enzyme was stored at −20°C or −80°C in the presence of 10% glycerol. Protein from each step of the purification was examined by SDS-PAGE for purity.

Determination of Physical Properties. Apo-SHMTs were prepared by the removal of thiazolidine formed between L-Cys and active site PLP. The same principle was used to determine the stoichiometry of PLP bound per molecule of enzyme with an extinction coefficient of 5580 M^{-1} cm^{-1} for thiazolidine (Ulevitch and Kallen, 1977). The quaternary structure was determined on a Superdex 200 size-exclusion column as described previously (Chang et al., 2006). The molar absorptivity coefficient was determined as stated previously by Gill and von Hippel (1989).

Enzyme Assays and Inhibition. The rate of N^5,N^{10}-CH_2-THF formation catalyzed by SHMT can be continuously monitored at 340 nm by coupling with excess N^5,N^{10}-CH_2-THF dehydrogenase, which converts $NADP^+$ to NADPH. All kinetic constants were determined in 20 mM potassium phosphate buffer, pH 7.0, containing 0.4 mM $NADP^+$, 5 mM 2-mercaptoethanol, and 0.5 μM methylenetetrahydrofolate dehydrogenase at 30°C in a 1-cm cuvette. These studies include determination of k_{cat} and K_m values for substrates, and inhibition by MTX and N^5-CHO-THF. L-Serine concentrations used in k_{cat} and K_m determination varied from 0.07 to 0.75 mM in the presence of 0.15 mM THF. Reactions were initiated by adding 10 μg of SHMT. Inhibition of initial velocity was determined in a 1-ml cuvette containing 20 mM phosphate, pH 7.3, 0.1 μM SHMT, 25 μM THF, 10 mM or 50 μM L-serine, saturated $NADP^+$, and inhibitors ranging from 0.1 to 100 μM for both N^5-CHO-THF and methotrexate.

Determination of Dissociation Constant for Reduced Folates. The dissociation constants for THF and N^5-CHO-THF of zmSHMT(DelSig) were measured by the formation of quinonoid complex in the presence of saturated glycine and reduced folates ranging from 2.5 to 54 μM (Strong et al., 1989; Chang et al., 2006). Results were analyzed with Scatchard plots and double-reciprocal plots, yielding K_d and stoichiometry of bound folates.

Fish Tissue Homogenization. Tissues or organs, including brain, eye, heart, liver, gastrointestinal tract, and muscle, were obtained from adult zebrafish after the animals were euthanized by waterborne exposure to tricaine (ethyl 3-aminobenzoate, methanesulfonic acid; Sigma-Aldrich). Tissues were rapidly isolated, stored in 50 to 200 μl of phosphate-buffered saline, pH 7.2, and kept on ice during the whole process of extraction. Homogenization was carried out in the phosphate-buffered saline lysis buffer containing a protease inhibitor cocktail consisting of AEBSF (aprotinin, leupeptin, bestatin, pepstatin A, and E-64) (Sigma-Aldrich, product number P8340) and RNase inhibitor (Recombinant RNasin; Promega, Madison, WI). Homogenized samples were centrifuged at 10,000*g* at 4°C for 10 min to remove particulate matter. Aliquots of the supernatant, about 10 to 30 μl, were subjected to Western blot and RT-PCR.

Western Blot Analysis. Supernatant protein content was determined using the Bradford (1976) and BCA methods. Proteins of 20 μg were separated on a 10% SDS-separating gel and transferred to a PVDF membrane (Millipore). After blocking in blocking solution containing 5% nonfat milk, 0.1% Tween 20 in phosphate-buffered saline overnight, the membrane was probed with anti-zcSHMT or anti-hmSHMT primary antibodies (1:1000–1:5000) and then horseradish peroxidase-conjugated secondary antibody (1:5000). The PVDF membranes were also probed with anti-actin antibody for a loading control. The membrane was visualized using the SuperSignal chemiluminescent horseradish peroxidase substrate system from Pierce on a FUJIFILM LAS-3000 imaging system (Fuji Film, Tokyo, Japan). In the case of the gastrointestinal tract, where the signal for actin was not detectable, Ponceau-S staining was used to verify equal loading.

We used the antibody against human mSHMT instead of zebrafish mSHMT to determine zmSHMT tissue distribution, owing to the concern of possible cross-reaction between zmSHMT and zcSHMT. The human mSHMT peptide sequence is 59% and 76% identical to zcSHMT and zmSHMT, respectively. The identity between zcSHMT and zmSHMT is 61%. Thus, we hoped that the hmSHMT antibody would clearly distinguish zmSHMT from zcSHMT. As expected, no cross-reaction was detected, even when we tested with 1 μg of purified proteins, allowing the uses of the antibodies as described.

RT-PCR Analysis. For RT-PCR determination of SHMT expression, total mRNA was isolated from tissues using a TRIzol kit (Invitrogen), following the manufacturer's instructions. After isolation, 1 μg of total mRNA in each tissue sample was reverse-transcribed with a high-capacity cDNA archive kit (Promega), and 1 μl of the newly synthesized first-strand cDNA library was used as template in the subsequent PCR analysis. The primer sequences are as follows: 5′- GGAGAGTCTGATTAATCAGGC -3′(F) and 5′- CATTTTGAGCCAGTTCCTCC -3′(R) for zcSHMT (505-bp fragment), 5′-GGAGAAGGTCAACTTC -3′(F) and 5′-GCGATTCGAGAAACCG -3′(R) for zmSHMT (523-bp fragment), and 5′-AGACATCAAGGAGAAGCTGTG-3′(F) and 5′-TCCAGACGGAGTATTTAC-3′(R) for β-actin (391-bp fragment) as a control for the RNA isolation and reverse-transcription. The annealing temperatures were 65°C for zcSHMT, 60°C for zmSHMT, and 62°C for β-actin. The PCR condition was 30 cycles of 30 s at 94°C, 30 s at annealing temperature, and 68°C for 30 s.

Determination of Intracellular Localization. ZLE cells were cultivated and regularly maintained in Leibovitz's L-15 medium supplemented with 5% fetal bovine serum at 28°C. For transient transfection, ZLE cells at 1 × 10^5/ml were subcultured into six-well plates 24 h before transfection with zSHMTs/pEGFP-N1 fusion plasmids with a si-PORT transfection kit (Ambion, Austin, TX). Cells were incubated for another 24 h and costained with mitochondrial probe MitoTracker Deep Red 633 (Invitrogen) right before examining under a confocal microscope. Confocal microscopy images were acquired on a Leica TCS SP2 microscope.

Results

Cloning and Sequence Analysis of Recombinant zmSHMT. The sequences of the 370-base pair fragments resulting from PCR amplification with degenerate primers fall into two categories, designated as form I and form II. We had previously reported the cloning and characterization of zSHMT form I, the prospective zcSHMT, which highly resembles mammalian cytosolic SHMT structurally and functionally (Chang et al., 2006). The full-length zSHMT form II cDNA isolated is 1479 bp, which encodes a protein of 492 amino acids. Peptide sequence alignment with the known SHMT from other species and the prospective zcSHMT revealed a potential mitochondrial signal peptide cleavage site between residues 20 and 30. Signal peptide prediction using the software SignalP 3.0 (http://www.cbs.dtu.dk/services/) has narrowed the cleavage site down to Ala22 and Val24, and is in agreement with the reports for rabbit and human

FIG. 2. Alignment of SHMT peptide sequences. The shaded characters indicate identical amino acids. Gaps, indicated by hyphens, are introduced for optimal alignment. The arrowhead indicates the conserved lysine residue that is in a highly conserved octapeptide threonine stretch and forms the internal aldimine with PLP. The arrow indicates the first residue in zmSHMT(DelSig). The sequences were aligned using the Clustal W method (Combet et al., 2000) with MegAlign/DNAstar sequence analysis software (DNASTAR, Madison, WI). The identities shared between zmSHMT and human and rabbit mitochondrial SHMT are 75.4% and 76.0%, respectively. The GenBank accession numbers of the aligned sequences are: human cytosolic SHMT, NP_004160; human mitochondrial SHMT, NP_005403; rabbit cytosolic SHMT, P07511; rabbit mitochondrial SHMT, P14519; zebrafish cytosolic SHMT, NP_957340; and zebrafish mitochondrial SHMT, EF213101.

mitochondrial SHMTs (Fig. 2) (Martini et al., 1989; Stover et al., 1997). This prospective mitochondrial leader sequence of zSHMT form II (which we now designate as zmSHMT) is rich in arginine, leucine, threonine, and serine, and fulfills the criteria for a mitochondrial targeting sequence that locates at the N terminus of the precursor protein and contains 17 to 35 amino acids rich in positive charge. Both the conserved octapeptide encompassing a stretch of threonine residues and the lysine residue forming the internal aldimine with PLP are also identified in zmSHMT, further supporting the notion that zebrafish SHMTs are the orthologs of mammalian SHMTs (Fig. 2). The peptide sequence of zmSHMT is 76% identical to its human ortholog, indicating a high conservation throughout evolution.

Expression and Purification of zSHMTs. The overexpressed full-length zmSHMT with leader peptide resulted in the formation of insoluble precipitate in *E. coli* at all the growth conditions we had tested, including lower temperatures, reduced inducer concentrations, and addition of cofactor PLP and low molecular weight glycols (data not shown). The attempt to obtain a soluble and fully functional protein succeeded only after we performed a second PCR-based cloning to eliminate the predicted leader peptide that includes the first 23 amino acids. Induction for zmSHMT without signal peptide, designated as zmSHMT(DelSig), reaches an acceptable level with minimal production of insoluble enzyme (Fig. 3). Higher concentrations of IPTG, elevated induction temperature, and/or prolonged induction time were found to increase the ratio of insoluble to soluble zmSHMT(DelSig), although the overall amount of induced enzyme is increased.

A purification protocol similar to those for zcSHMT and human SHMTs was applied to the purification for zmSHMT(DelSig) (Kruschwitz et al., 1995; Chang et al., 2006). After a 30 to 50% ammonium sulfate precipitation, the enzyme was 70% pure, judged from SDS-PAGE, with a 2-fold purification (Table 1). We used gel filtration, instead of equilibrium dialysis, to remove ammonium sulfate, because zmSHMT(DelSig) was found to precipitate after overnight dialysis. The zmSHMT(DelSig) bound to CM-Sephadex and was eluted at high salt. Chromatographing on CM-Sephadex separates the endogenous enzyme from our cloned zmSHMT, since most *E. coli* proteins, including *E. coli* SHMT, do not bind to cation exchange resins under

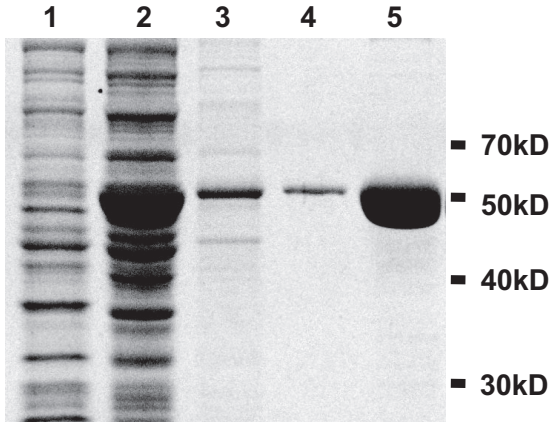

FIG. 3. SDS-PAGE of zmSHMT(DelSig) at each step of purification. Lane 1, lysate of cells without induction; lane 2, lysate of cells induced with IPTG; lane 3, after ammonium sulfate precipitation; lane 4, after CM column; lane 5, overloaded purified zmSHMT(DelSig).

these conditions (di Salvo et al., 1998). Therefore, this step greatly simplifies the purification procedure and permits removal of the great bulk of unwanted protein, with a large -fold of purification achieved. The SHMT eluted from this column was better than 98% pure (Fig. 3). From 2 liters of cells, approximately 43 mg of pure zmSHMT(DelSig) was obtained with an overall yield of 90% (Table 1). The purified recombinant enzyme can be stored at −20°C or −80°C in the presence of 10% glycerol for at least 6 months without significant change in catalytic activity. However, frequent freeze-thaw cycles result in protein precipitation and loss of enzymatic activity.

Physical Properties of zmSHMT(DelSig). The spectral properties of the recombinant zmSHMT(DelSig) seem to be similar to those of most of the studied SHMTs, including human (Kruschwitz et al., 1995; di Salvo et al., 1998; Chang et al., 2006). Beside 278 nm, zmSHMT (DelSig) displays a distinct absorbance peak at 428 nm, corresponding to the internal aldimine formed between PLP and an active site lysine residue (Fig. 4). The 428-nm peak in all other studied SHMTs gives a distinct spectral change in the presence of glycine and reduced folates due to the formation of a quinonoid ternary complex absorbing near 500 nm. This long wavelength absorbance is attributed to a glycine anion in resonance with the bound pyridoxal phosphate and has been used extensively to determine the binding constants of tetrahydrofolates and glycine (Schirch, 1982). The same properties were observed for the recombinant zmSHMT(DelSig) (Fig. 4).

The predicted molar absorptivity coefficient at 278 nm for denatured zmSHMT(DelSig) was 39,910 M^{-1} cm^{-1}, based on amino acid composition. The coefficient of the native enzyme was obtained by multiplying the predicted value by the ratio of absorbance at 278 nm for denatured and native states, yielding a molar absorptivity coefficient of zmSHMT(DelSig) ε_{278} = 45,893 M^{-1} cm^{-1}. This shows that a 1-mg/ml solution of zmSHMT(DelSig) holoenzyme will exhibit absorption of 0.88 at 278 nm. This level is slightly higher, but comparable to that of zcSHMT, which has a molar absorptivity coefficient of 45,060 M^{-1} cm^{-1} (Chang et al., 2006). The Trp residues contained in zcSHMT and zmSHMT are two and three, respectively.

SDS-PAGE showed a single band of approximately 50 kDa for the recombinant zmSHMT(DelSig) (Fig. 3). This compares to the calculated size of 51,912 Da based on the peptide sequence of a zmSHMT(DelSig) monomer. Both holo- and apo-zmSHMT(DelSig) had a Stokes radius close to a globular protein of 200 kDa and were eluted at the same retention volume as zcSHMT and human cytosolic SHMT tetramers on a Superdex 200 column (data not shown). These results suggest a homotetrameric structure for the recombinant zmSHMT(DelSig).

L-Cysteine forms a thiazolidine compound with the active site PLP, which can be removed by dialysis or precipitation of the protein, providing a simple method for preparing mitochondrial apo-SHMT and determination of PLP binding stoichiometry (Ulevitch and Kallen, 1977). Our results show that one PLP molecule binds to each zmSHMT(DelSig) monomer, as observed for zcSHMT and most of the SHMTs studied to date (data not shown).

Steady-State Kinetic Constants and Reduced Folate Affinity. Double-reciprocal plots of initial velocity versus serine concentration permit the determination of both apparent K_m for serine and k_{cat}. As shown in Table 2, both the K_m of serine and the k_{cat} of zmSHMT(DelSig) are comparable to the values for zcSHMT and rabbit mitochondrial SHMT. The enzyme remains fully active at 37°C for at least 30 min (data not shown).

The quinonoid intermediate formed between reduced folates and the active site PLP absorbs near 500 nm with a molar extinction coefficient of 40,000 M^{-1} cm^{-1} (Schirch et al., 1977). This absorbance shows saturation kinetics with most reduced folate substrates, including $H_4PteGlu_n$, N^5-CHO-$H_4PteGlu_n$, and N^5-CH_3-$H_4PteGlu_n$ (Schirch and Ropp, 1967; Stover and Schirch, 1991). The binding of substrates to rabbit cytosolic SHMT is a sequential random mechanism. Previous studies had confirmed that the K_d values determined by this method were essentially the same as the K_m for folate determined from kinetic measurements (Schirch et al., 1977; Szebenyi et al., 2004). However, the reported value is an apparent K_d because the formation of this complex is at least a two-step process. The lower K_d of zmSHMT(DelSig) for THF suggests a higher affinity for this substrate compared with zcSHMT. Both isoforms have comparable affinity for N^5-CHO-THF, as judged from their similar dissociation constants (Table 2).

Inhibition of SHMT Aldol Cleavage Activity. Increasing concentrations of leucovorin (N^5-CHO-THF) inhibit both zcSHMT and hcSHMT activities substantially, yet to a lesser extent than zmSHMT (Fig. 5). The inhibitions of SHMT-catalyzed serine aldol cleavage by leucovorin and MTX were determined for zc-, zm-, and hcSHMT. Approximately 70% and 30% inhibition were observed for zc- and zmSHMT(DelSig) activities, respectively, in the presence of 70 μM N^5-CHO-THF (Fig. 5A). The IC_{50} of leucovorin is approximately 30 μM for zcSHMT and higher than 70 μM for zmSHMT. The differential inhibition is evident with the presence of 10 μM leucovorin, the concentration estimated in serum in a high-dose leucovorin rescue regimen. A similar pattern of inhibition, but an even larger difference between zc- and zmSHMT was observed when the inhibition was assayed in the presence of 50 μM serine (Fig. 5B). MTX also represses SHMT activities, but not as significantly as it does zebrafish DHFR activity (Fig. 5C; T. F. Fu, unpublished result). No significant difference was observed when the highest concentrations of leucovorin (70 μM) and MTX (100 μM) were added simultaneously to the reaction in a combined assay compared with adding leucovorin alone (data not shown).

Tissue-Specific Distribution of zmSHMT and zcSHMT Isoforms. RT-PCR results showed that zmSHMT mRNA was evenly distributed among tissues, whereas significantly higher levels of zcSHMT mRNA were detected in heart, liver, and ova (Fig. 6C). This result is in agreement with the ubiquitous distribution of human mSHMT message and tissue-specific expression of cSHMT mRNA (Girgis et al., 1998). PCR was also performed using plasmids containing zcSHMT or zmSHMT coding sequences as templates to

TABLE 1

Summary of recombinant zmSHMT(DelSig) purification

Step	Volume (ml)	Protein (mg)	Total Activity (U)	Specific Activity (U/mg)	Yield (%)	Purification (fold)
Cell lysate	19	537	736	1.37	100	1
$(NH_4)_2SO_4$	15	297	825	2.77	120	2
CM	2	43	658	15.3	90	11.2

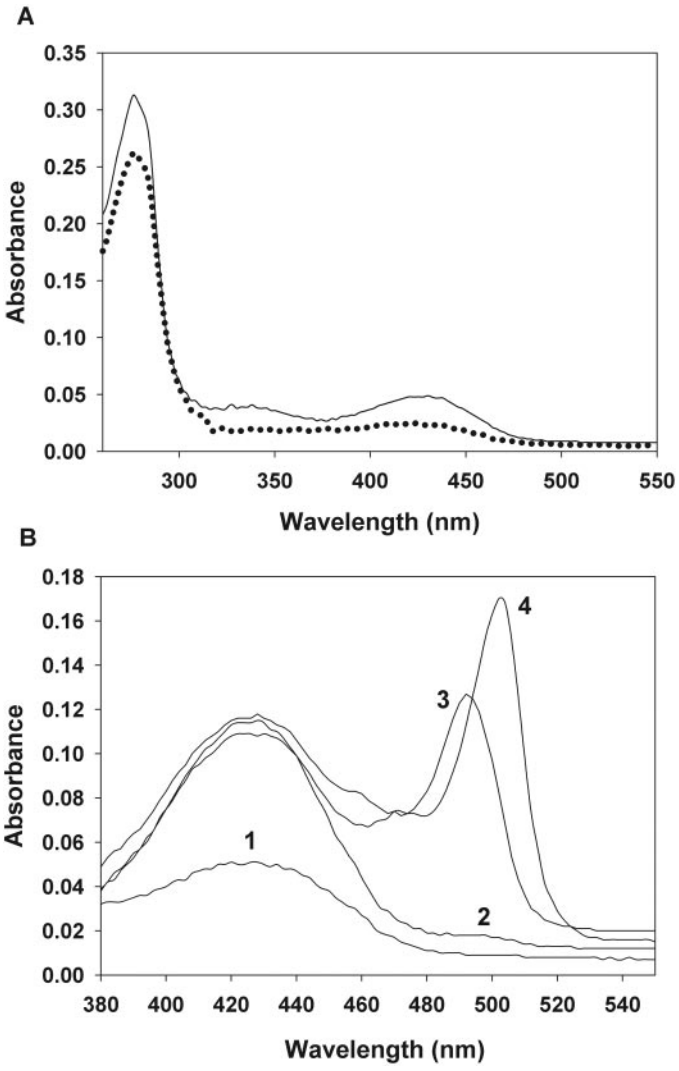

FIG. 4. Absorbance of zebrafish SHMTs and its complexes with glycine and folate substrates. A, spectrum of zcSHMT (solid line) and zmSHMT(DelSig)(dotted line) in 20 mM potassium phosphate at pH 7.0. B, spectrum of zmSHMT(DelSig) (curve 1), zmSHMT(DelSig) saturated with glycine (curve 2), zmSHMT(DelSig) saturated with glycine and H_4PteGlu (curve 3), and zmSHMT(DelSig) saturated with glycine and N^5-CHO-H_4PteGlu (curve 4).

validate the positive signal. No PCR product was observed in this cross-reaction test (Fig. 6A).

Interestingly, we found that the SHMT protein levels did not correspond to their mRNA amounts detected in most of the tissues examined. Strong tissue specificity was observed in protein levels for both zcSHMT and zmSHMT (Fig. 6C). Zebrafish cSHMT protein was predominant in liver and also abundant in ova. Significant zmSHMT protein was detected only in liver and gastrointestinal tract regardless of the evenly distributed mRNA message. We also noted that appreciable amounts of cSHMT, but not mSHMT, were found in unfertilized eggs in both mRNA and protein levels. Equal loading of samples was confirmed by the presence of β-actin, Ponceau-S staining of the membrane, and Coomassie Brilliant Blue-stained SDS-polyacrylamide gel.

Subcellular Localization of Zebrafish SHMTs. The prediction on the recombinant zSHMT's intracellular localization was confirmed by the site-specific compartmentalization of EGFP-fused SHMTs with confocal microscopy. The overexpressed zmSHMT-EGFP was clearly colocalized with a mitochondrial marker, demonstrating the mitochondrial localization of this enzyme (Fig. 7A). For zcSHMT-EGFP, surprisingly, the fluorescence signal of various intensities was detected in both nucleus and cytosol. No signal corresponding to free GFP was detected in cell extracts prepared from zcSHMT-EGFP transformants, excluding the possibility of artifacts or false signal due to any undesired sample contamination (Fig. 7B).

Discussion

Despite the unknown biological function and significance of SHMTs, studies showed that impairment of SHMT activity resulted in disturbance of homeostasis of the intracellular one-carbon pool and led to pathogeneses including homocysteinemia, cancers, cardiovascular diseases, and neural tube defects, implying a crucial role of SHMT in normal cell growth and functions (Stover and Garza, 2006). The existence of both cytosolic and mitochondrial SHMTs has been known since Nakano et al. (1968) partially purified the enzyme from rat liver mitochondria in 1968. Since then, cytosolic SHMTs of many species have been studied thoroughly, whereas information about the mitochondrial isoform is still very limited.

We report here the cloning and characterization of zebrafish mitochondrial SHMT. The identity of this recombinant protein was confirmed by its serine-aldol cleavage activity and colocalization with MitoTracker Red, a mitochondrial specific dye. The full-length zmSHMT expressed in *E. coli* forms inclusion bodies. This result was not unexpected since expression of organelle-specific proteins containing signal peptide often leads to formation of insoluble protein. Further characterization of zmSHMT(DelSig) reveals substantial similarities in its structure, physical properties, and kinetics to zcSHMT and mammalian orthologs, adding confidence to using zebrafish as an animal model for folate-related studies. That similar protocols applied to the purification of hcSHMT, rcSHMT, zcSHMT, and zmSHMT(DelSig) suggests comparable surface properties among these isoforms. Surprisingly, no evident cross-reaction between anti-zcSHMT antibody and zmSHMT(DelSig) protein was detected in Western blot analysis, despite a 63% identity being found in their peptide sequences. The possible explanation is that the homologous sequences might be embedded inside and therefore were not exposed to lymphocyte recognition and antibody generation.

It is interesting to note that the aldol cleavage of serine catalyzed by zc- and zmSHMTs was differentially inhibited by N^5-CHO-THF (leucovorin), despite both enzymes binding to this compound with similar affinity. To our knowledge, this is the first report on the effect of leucovorin on mitochondrial SHMT. The concentrations of serine and THF used in the inhibition assays encompassed the physiological concentrations of both substrates, implying that the similar inhibition

TABLE 2

Comparison of kinetic parameters for recombinant zmSHMT(DelSig) with zcSHMT and rmSHMT

Apparent K_m and V_{max} values were determined by fitting the data to the Michaelis-Menten equation using Sigma Plot.

Species	αK_m for serine (mM)	αK_d for H_4PteGlu (μM)	αK_d for N^5-CHO-H_4PteGlu (μM)	Turnover Number (min^{-1})	References
Zebrafish m[a]	0.43	8	2.8	537	Present report
Zebrafish c[b]	0.22	18	2.6	351	Chang et al. (Chang et al., 2006)
Rabbit m[c]	0.60	25	10	500	Schirch et al. (Schirch and Peterson, 1980)

[a] zebrafish mSHMT(DelSig); [b] cytosolic SHMT; [c] mitochondrial SHMT

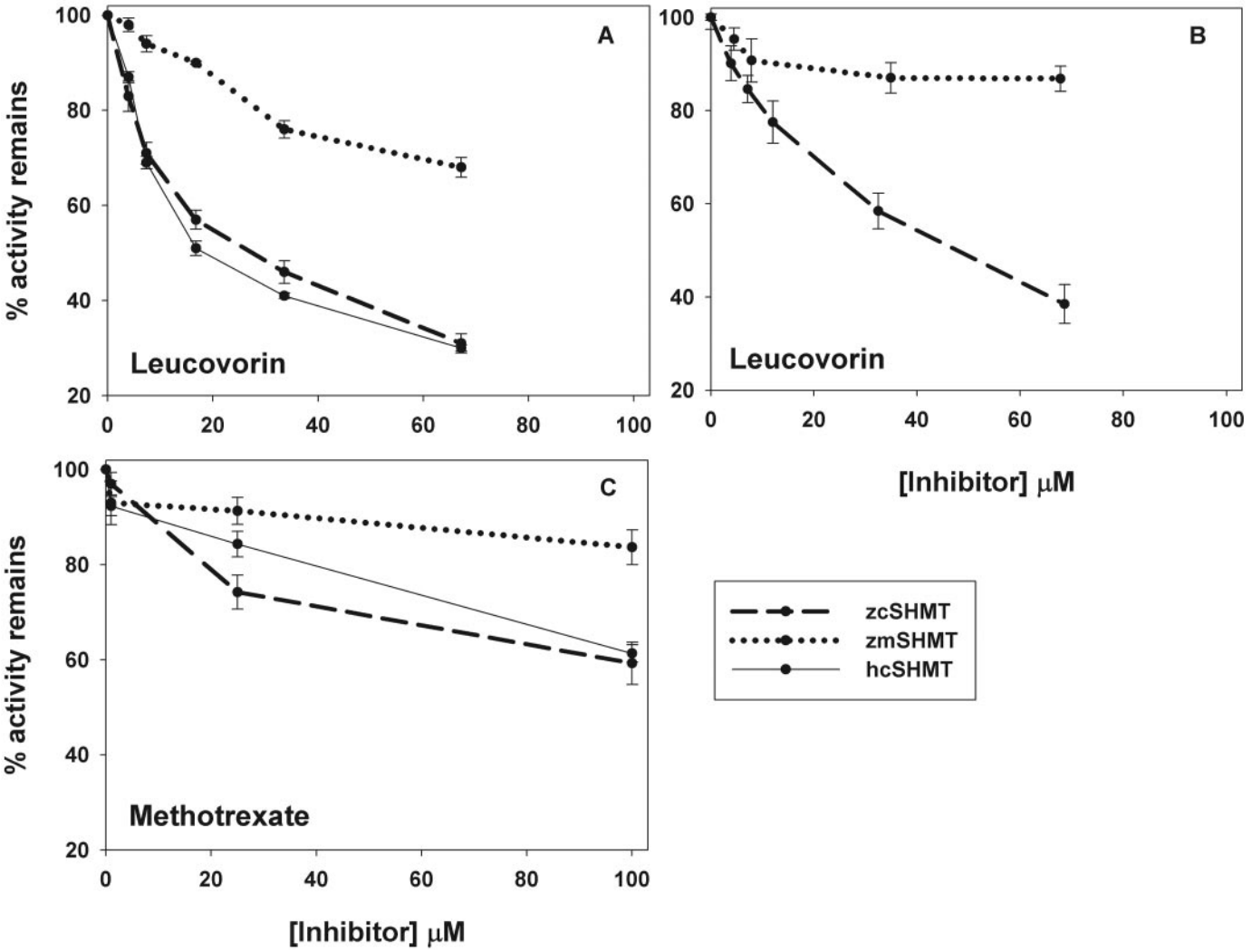

FIG. 5. Inhibition of the SHMT-catalyzed serine-aldol cleavage by increasing concentrations of leucovorin (N^5-CHO-THF) (A and B) and methotrexate (C). Inhibition on initial velocity was determined at 30°C in the presence of 25 μM H_4PteGlu, saturated $NADP^+$, 10 mM (A and C) or 50 μM (B) serine, 0.1 μM SHMT, and inhibitors ranging from 0.1 to 100 μM.

pattern might also occur in vivo (Vinnars et al., 1975). The differential inhibition observed between these two isoforms might be attributed to the lower K_d of zmSHMT than of zcSHMT for THF. Stover and colleagues suggested that N^5-CHO-THF binds and modulates cSHMT activity, enabling this enzyme to function as a regulatory switch in one-carbon metabolism. When activated, the cSHMT-derived N^5,N^{10}-CH_2-THF gives the thymidylate synthetic pathway higher metabolic priority than the homocysteine remethylation cycle (Herbig et al., 2002; Woeller et al., 2007). The latter one generates *S*-adenosyl methionine, the major methyl donor for most intracellular methylation including DNA and protein. Our results add further weight to the notion that zmSHMT is responsible for a stable supply of N^5,N^{10}-CH_2-THF, whereas cSHMT is sensitive to alteration in nutritional status and functions to regulate the one-carbon flow in a changed environment (Stover and Garza, 2006). In a high-dose MTX combined leucovorin rescue therapy, the differential inhibitory effects of N^5-CHO-THF to zc- and zmSHMT might result in a decreased ratio of THF to N^5,N^{10}-CH_2-THF, and hence, redistribution of the activated one-carbon units between nucleotide biosynthesis and cellular methylation, yielding profound impact in intracellular events, gene activities, and, ultimately, cell survival. Evidence supporting the notion that cSHMT activity might play a role in the development of MTX

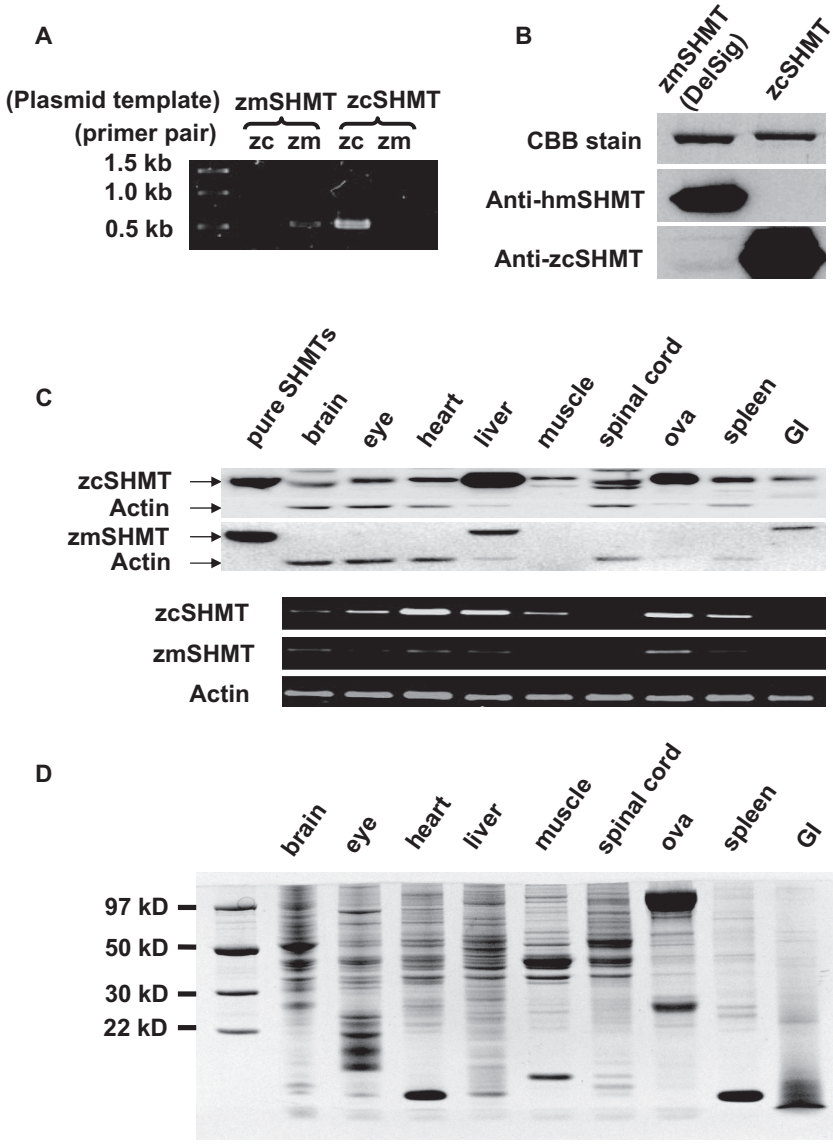

FIG. 6. Tissue distribution of zebrafish cytosolic and mitochondrial SHMTs. A, plasmids (20 ng) containing SHMT coding sequences were used as templates in PCRs for specificity determination with the primer pairs indicated. B, anti-zcSHMT and anti-hmSHMT antibodies were tested against purified zcSHMT and zmSHMT for specificity. One microgram of each purified protein was subjected to SDS-PAGE and analyzed by Coomassie Brilliant Blue (CBB) staining (top) and Western blotting with anti-hmSHMT (middle) and anti-zcSHMT (bottom) antibodies. C, individual tissues were prepared for Western blot (top) and RT-PCR (bottom) analysis from adult female zebrafish as described under *Materials and Methods*. D, tissue extracts containing 20 μg of protein were separated by 10% SDS-PAGE and visualized by Coomassie Brilliant Blue staining. Results presented here are representative of six independent repeats. GI, gastrointestinal.

resistance has been reported. In support of this notion are that polymorphism in cSHMT was related to MTX resistance in pediatric patients with acute lymphoblastic leukemia, and overexpression of cSHMT in *Leishmania* increased resistance to methotrexate in a rich folate-containing medium (de Jonge et al., 2005; Gagnon et al., 2006). The present study adds mSHMT to the picture for possible mechanistic insights and provides clues to further understand the complex relationships between one-carbon metabolism, SHMTs, and the development of MTX resistance.

The MTX and leucovorin concentrations used in the inhibition studies ranged from 0.1 to 100 μM. It was estimated that a concentration of 1 to 10 μM for both MTX and leucovorin is a realistic serum concentration that can be reached in a MTX-leucovorin combined regimen (Widemann and Adamson, 2006). However, we are convinced that the differential inhibition observed in our studies should have reflected what has occurred in vivo, since the polyglutamylation of folate/antifolate substrates will significantly increase their affinities to folate enzymes. Five to seven glutamate residues will be added to the γ-carboxyl group of the internalized MTX and N^5-CHO-THF. Studies showed that the K_d values of rabbit cSHMT were close to 5 μM for both $H_4PteGlu_1$ and N^5-CHO-$H_4PteGlu_1$, whereas the K_d values of the same enzyme are 0.056 and 0.02 mM for $H_4PteGlu_5$ and N^5-CHO-$H_4PteGlu_5$, respectively (Huang et al., 1998; Fu et al., 2005). This result implies that the inhibition mediated by N^5-CHO-$H_4PteGlu_5$ in cells should be comparable to, if not more significant than, the results observed in in vitro studies since polyglutamylation will further potentiate the competitiveness of polyglutamylated leucovorin with tetrahydrofolate polyglutamate.

Tissue-specific expression was evident in the protein level for both SHMT isozymes in zebrafish, with the highest expression in liver. This is, to our knowledge, the first report on the tissue-specific distribution of mitochondrial SHMT. It was documented that human mSHMT mRNA was evenly expressed among tissues (Girgis et al., 1998). Interestingly, our RT-PCR results for zmSHMT were in agreement with the human mSHMT expression pattern and showed equal distribution, suggesting that translational and/or post-translational regulation might play a role in controlling the intracellular concentrations of both enzymes. Protein stabilized by the binding of folate substrates and/or PLP cofactor might also contribute to the different protein levels observed in this study. Support for this notion is very recent, showing that lack of vitamin B_6 in cells causes a decrease in SHMT protein but not mRNA level (Perry et al., 2007). Notably, cSHMT is abundant in unfertilized eggs, supporting the view that SHMT is a maternally essential gene (Vatcher et al., 1998). Studies on the cor-

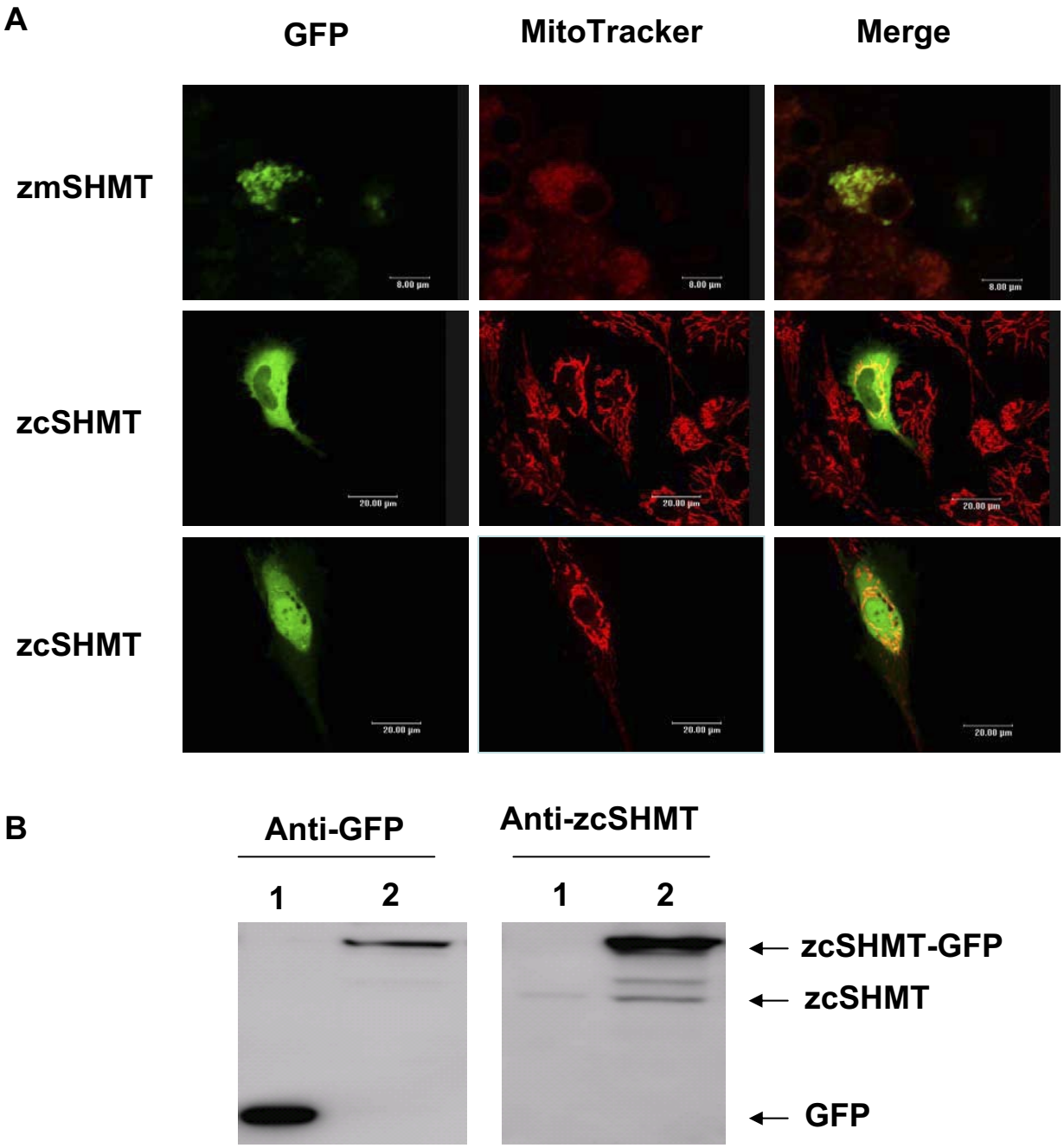

FIG. 7. Localization of EGFP-tagged zSHMTs in ZLE cells. A, the EGFP fusion constructs with zmSHMT (top) or zcSHMT (middle and bottom) fused to the N terminus of EGFP were transiently transfected into ZLE cells, and live confocal images were taken at 24 h after transfection. The scales at the lower right corner for zmSHMT-EGFP and zcSHMT-EGFP transformants are 8.00 μm and 20.00 μm, respectively. B, extracts containing 20 μg of protein prepared from cells transfected with plasmid generating free EGFP (lane 1) or zcSHMT-EGFP fusion protein (lane 2) were subjected to 10% SDS-PAGE and Western blot analysis with antibodies indicated on the top.

relation between the abundance of SHMTs and the potential risk of developing MTX resistance might be rewarded by an understanding of the differential efficacy of MTX observed in various types of cancer.

We were puzzled and vigilant when we observed the presence of zcSHMT in the nucleus, since the nuclear localization of cSHMT had never been reported at that time. A negative result was obtained when the peptide sequence was subjected to a search for a specific nuclear-targeting sequence. Having repeated this experiment carefully and revealed the same results many times prompted us to postulate that the zcSHMT-EGFP might be transported into nucleus via cargo or other component-mediated mechanisms. Interestingly, our observation and hypothesis were found later to be in agreement with what was reported by Woeller et al. (2007) in a very recent study showing that human cSHMT was SUMOylated and nuclear-localized in a cell cycle-dependent manner. Two prospective SUMOylation sites are identified in the zcSHMT peptide sequence, suggesting a possibly similar mechanism for zcSHMT nuclear localization and a resemblance between human and zebrafish SHMTs. The biological significance of the nuclear-localized cSHMT is unknown. Yang and Meier (2003) showed that cSHMT was in some way connected to the nucleolar protein SRP40p and modulated cell cycle and cell size, supporting a noncatalytic function of cSHMT. Enlargement of the cell size was also observed in our zcSHMT-EGFP-transfected cells. The

significance of zcSHMT intracellular localization is currently under investigation.

Zebrafish have attracted the interest of many researchers as an animal model in the past two decades. The features of external development, transparent embryo, ease of growth and breeding, economy, and ease of manipulation using well established molecular approaches have made zebrafish an ideal animal model for studying developmental biology and pathogenic mechanisms in a variety of conditions. Especially important for drug discovery is that zebrafish embryos are permeable to small molecules and drugs during organogenesis, providing easy access for drug administration and vital dye staining (Kari et al., 2007). There is no doubt that efforts will be continually invested in the improvement of antifolate drugs, considering the vital role of folates in nucleotides and protein biosynthesis. The search for new targets of antifolate drugs will also be sustained. In addition to its vital role in folate-mediated one-carbon metabolism, the property of being highly expressed in rapidly proliferating cells has made SHMT a potential target for chemotherapy and immunosuppression (Renwick et al., 1998). Our studies conclude that zebrafish SHMTs share high similarity with human isozymes, indicating that zSHMTs, and probably zebrafish as a whole, are appropriate systems for folate-related studies and antifolate drug discovery. Further studies on other folate enzymes should be warranted. In addition, the possible mechanistic insights provided in this study enable us to further understand the complex relationships between one-carbon metabolism, SHMTs, and the development of MTX resistance.

Acknowledgments. Our sincere appreciation goes to Dr. Verne Schirch, Virginia Commonwealth University, for valuable advice and assistance. We also thank Dr. R. Moser, Merck Eprova AG, and Dr. Jiann-Ruey Hong, National Cheng Kung University, for the precious materials they generously provided.

References

Appling DR (1991) Compartmentation of folate-mediated one-carbon metabolism in eukaryotes. *FASEB J* **5:**2645–2651.

Asai S, Miyachi H, Kobayashi H, Takemura Y, and Ando Y (2003) Large diversity in transport-mediated methotrexate resistance in human leukemia cell line CCRF-CEM established in a high concentration of leucovorin. *Cancer Sci* **94:**210–214.

Bleyer WA (1977) Methotrexate: clinical pharmacology, current status and therapeutic guidelines. *Cancer Treat Rev* **4:**87–101.

Bradford MM (1976) A rapid and sensitive method for the quantitation of microgram quantities of protein utilizing the principle of protein-dye binding. *Anal Biochem* **72:**248–254.

Chang WN, Tsai JN, Chen BH, and Fu TF (2006) Cloning, expression, purification, and characterization of zebrafish cytosolic serine hydroxymethyltransferase. *Protein Expr Purif* **46:**212–220.

Combet C, Blanchet C, Geourjon C, and Deleage G (2000) NPS@: network protein sequence analysis. *Trends Biochem Sci* **25:**147–150.

de Jonge R, Hooijberg JH, van Zelst BD, Jansen G, van Zantwijk CH, Kaspers GJ, Peters GJ, Ravindranath Y, Pieters R, and Lindemans J (2005) Effect of polymorphisms in folate-related genes on in vitro methotrexate sensitivity in pediatric acute lymphoblastic leukemia. *Blood* **106:**717–720.

di Salvo ML, Delle FS, De BD, Bossa F, and Schirch V (1998) Purification and characterization of recombinant rabbit cytosolic serine hydroxymethyltransferase. *Protein Expr Purif* **13:**177–183.

Frei E III, Blum RH, Pitman SW, Kirkwood JM, Henderson IC, Skarin AT, Mayer RJ, Bast RC, Garnick MB, Parker LM, et al. (1980) High dose methotrexate with leucovorin rescue. Rationale and spectrum of antitumor activity. *Am J Med* **68:**370–376.

Fu TF, Hunt S, Schirch V, Safo MK, and Chen BH (2005) Properties of human and rabbit cytosolic serine hydroxymethyltransferase are changed by single nucleotide polymorphic mutations. *Arch Biochem Biophys* **442:**92–101.

Gagnon D, Foucher A, Girard I, and Ouellette M (2006) Stage specific gene expression and cellular localization of two isoforms of the serine hydroxymethyltransferase in the protozoan parasite Leishmania. *Mol Biochem Parasitol* **150:**63–71.

Gill SC and von Hippel PH (1989) Calculation of protein extinction coefficients from amino acid sequence data. *Anal Biochem* **182:**319–326.

Girgis S, Nasrallah IM, Suh JR, Oppenheim E, Zanetti KA, Mastri MG, and Stover PJ (1998) Molecular cloning, characterization and alternative splicing of the human cytoplasmic serine hydroxymethyltransferase gene. *Gene* **210:**315–324.

Herbig K, Chiang EP, Lee LR, Hills J, Shane B, and Stover PJ (2002) Cytoplasmic serine hydroxymethyltransferase mediates competition between folate-dependent deoxyribonucleotide and S-adenosylmethionine biosyntheses. *J Biol Chem* **277:**38381–38389.

Horne DW, Holloway RS, and Said HM (1992) Uptake of 5-formyltetrahydrofolate in isolated rat liver mitochondria is carrier-mediated. *J Nutr* **122:**2204–2209.

Huang T, Wang C, Maras B, Barra D, and Schirch V (1998) Thermodynamic analysis of the binding of the polyglutamate chain of 5-formyltetrahydropteroylpolyglutamates to serine hydroxymethyltransferase. *Biochemistry* **37:**13536–13542.

Kari G, Rodeck U, and Dicker AP (2007) Zebrafish: an emerging model system for human disease and drug discovery. *Clin Pharmacol Ther* **82:**70–80.

Kimmel CB, Ballard WW, Kimmel SR, Ullmann B, and Schilling TF (1995) Stages of embryonic development of the zebrafish. *Dev Dyn* **203:**253–310.

Kruschwitz H, Ren S, Di SM, and Schirch V (1995) Expression, purification, and characterization of human cytosolic serine hydroxymethyltransferase. *Protein Expr Purif* **6:**411–416.

Marasas WF, Riley RT, Hendricks KA, Stevens VL, Sadler TW, Gelineau-van WJ, Missmer SA, Cabrera J, Torres O, Gelderblom WC, et al. (2004) Fumonisins disrupt sphingolipid metabolism, folate transport, and neural tube development in embryo culture and in vivo: a potential risk factor for human neural tube defects among populations consuming fumonisin-contaminated maize. *J Nutr* **134**:711–716.

Martini F, Maras B, Tanci P, Angelaccio S, Pascarella S, Barra D, Bossa F, and Schirch V (1989) The primary structure of rabbit liver mitochondrial serine hydroxymethyltransferase. *J Biol Chem* **264:**8509–8519.

Nakano Y, Fujioka M, and Wada H (1968) Studies on serine hydroxymethylase isoenzymes from rat liver. *Biochim Biophys Acta* **159:**19–26.

Narkewicz MR, Sauls SD, Tjoa SS, Teng C, and Fennessey PV (1996) Evidence for intracellular partitioning of serine and glycine metabolism in Chinese hamster ovary cells. *Biochem J* **313 (Pt 3):**991–996.

Perry C, Yu S, Chen J, Matharu KS, and Stover PJ (2007) Effect of vitamin B6 availability on serine hydroxymethyltransferase in MCF-7 cells. *Arch Biochem Biophys* **146:**21–27.

Renwick SB, Snell K, and Baumann U (1998) The crystal structure of human cytosolic serine hydroxymethyltransferase: a target for cancer chemotherapy. *Structure* **6:**1105–1116.

Schirch L (1982) Serine hydroxymethyltransferase. *Adv Enzymol Relat Areas Mol Biol* **53:**83–112.

Schirch L and Peterson D (1980) Purification and properties of mitochondrial serine hydroxymethyltransferase. *J Biol Chem* **255:**7801–7806.

Schirch L and Ropp M (1967) Serine transhydroxymethylase. Affinity of tetrahydrofolate compounds for the enzyme and enzyme-glycine complex. *Biochemistry* **6:**253–257.

Schirch LV, Tatum CM Jr, and Benkovic SJ (1977) Serine transhydroxymethylase: evidence for a sequential random mechanism. *Biochemistry* **16:**410–419.

Sirotnak FM, Moccio DM, and Dorick DM (1978) Optimization of high-dose methotrexate with leucovorin rescue therapy in the L1210 leukemia and sarcoma 180 murine tumor models. *Cancer Res* **38:**345–353.

Stover P and Schirch V (1991) 5-Formyltetrahydrofolate polyglutamates are slow tight binding inhibitors of serine hydroxymethyltransferase. *J Biol Chem* **266:**1543–1550.

Stover PJ, Chen LH, Suh JR, Stover DM, Keyomarsi K, and Shane B (1997) Molecular cloning, characterization, and regulation of the human mitochondrial serine hydroxymethyltransferase gene. *J Biol Chem* **272:**1842–1848.

Stover PJ and Garza C (2006) Nutrition and developmental biology—implications for public health. *Nutr Rev* **64:**S60–S71.

Strong WB, Cook R, and Schirch V (1989) Interaction of tetrahydropteroylpolyglutamates with two enzymes from mitochondria. *Biochemistry* **28:**106–114.

Szebenyi DM, Musayev FN, di Salvo ML, Safo MK, and Schirch V (2004) Serine hydroxymethyltransferase: role of glu75 and evidence that serine is cleaved by a retroaldol mechanism. *Biochemistry* **43:**6865–6876.

Ulevitch RJ and Kallen RG (1977) Purification and characterization of pyridoxal 5′-phosphate dependent serine hydroxymethylase from lamb liver and its action upon beta-phenylserines. *Biochemistry* **16:**5342–5350.

Vatcher GP, Thacker CM, Kaletta T, Schnabel H, Schnabel R, and Baillie DL (1998) Serine hydroxymethyltransferase is maternally essential in Caenorhabditis elegans. *J Biol Chem* **273:**6066–6073.

Vinnars E, Bergstom J, and Furst P (1975) Influence of the postoperative state on the intracellular free amino acids in human muscle tissue. *Ann Surg* **182:**665–671.

Westerfield M (2000) *The Zebrafish Book.* University of Oregon Press, Eugene.

Widemann BC and Adamson PC (2006) Understanding and managing methotrexate nephrotoxicity. *Oncologist* **11:**694–703.

Woeller CF, Anderson DD, Szebenyi DM, and Stover PJ (2007) Evidence for small ubiquitous modifier-dependent nuclear import of the thymidylate biosynthesis pathway. *J Biol Chem* **282:**17623–17631.

Yang Y and Meier UT (2003) Genetic interaction between a chaperone of small nucleolar ribonucleoprotein particles and cytosolic serine hydroxymethyltransferase. *J Biol Chem* **278:**23553–23560.

Address correspondence to: Tzu-Fun Fu, Department of Medical Laboratory Science and Biotechnology, College of Medicine, National Cheng Kung University, No.1, University Road, Tainan 701, Taiwan. E-mail: tffu@mail.ncku.edu.tw.